Food Chemistry 182 (2015) 275–281

Contents lists available at ScienceDirect

Food Chemistry

journal homepage: www.elsevier.com/locate/foodchem

Core–shell biopolymer nanoparticle delivery systems: Synthesis and characterization of curcumin fortified zein–pectin nanoparticles

Kun Hu [a], Xiaoxia Huang [a], Yongqing Gao [a], Xulin Huang [a], Hang Xiao [b], David Julian McClements [b,c,*]

[a] Food Science School, Guangdong Pharmaceutical University, Zhongshan 528458, China
[b] Department of Food Science, University of Massachusetts, Amherst, MA 01003, USA
[c] Department of Biochemistry, Faculty of Science, King Abdulaziz University, P.O. Box 80203, Jeddah 21589, Saudi Arabia

ARTICLE INFO

Article history:
Received 23 November 2014
Received in revised form 3 February 2015
Accepted 3 March 2015
Available online 11 March 2015

Keywords:
Curcumin
Zein
Pectin
Nanoparticles
Delivery system
Encapsulation

ABSTRACT

Biopolymer core–shell nanoparticles were fabricated using a hydrophobic protein (zein) as the core and a hydrophilic polysaccharide (pectin) as the shell. Particles were prepared by coating cationic zein nanoparticles with anionic pectin molecules using electrostatic deposition (pH 4). The core–shell nanoparticles were fortified with curcumin (a hydrophobic bioactive molecule) at a high loading efficiency (>86%). The resulting nanoparticles were spherical, relatively small (diameter ≈ 250 nm), and had a narrow size distribution (polydispersity index ≈ 0.24). The encapsulated curcumin was in an amorphous (rather than crystalline form) as detected by differential scanning calorimetry (DSC). Fourier transform infrared (FTIR) and Raman spectra indicated that the encapsulated curcumin interacted with zein mainly through hydrophobic interactions. The nanoparticles were converted into a powdered form that had good water-dispersibility. These core–shell biopolymer nanoparticles could be useful for incorporating curcumin into functional foods and beverages, as well as dietary supplements and pharmaceutical products.

1. Introduction

Curcumin is a natural lipophilic polyphenol found in the rhizomes of turmeric (*Curcuma longa*) (Kumar, Mahesh, Mahadevan, & Mandal, 2014). It has been used as a traditional medicine and as a food pigment in India and China for centuries. Recent research suggests that it may possess a broad range of pharmacological activities such as antioxidant, anti-inflammatory, antimicrobial, antiviral, antirheumatic, and neuroprotective properties (Anand, Kunnumakkara, Newman, & Aggarwal, 2007; Bhawana et al., 2011; Duvoix et al., 2005). Curcumin has also been shown to inhibit the viability and proliferation of a variety of human cancer cell lines including skin, gastrointestinal, genitourinary, breast, ovarian, and lung cancers (Anand et al., 2008; Jambhrunkar, Karmakar, Popat, Yu, & Yu, 2014). Despite its potential health benefits, curcumin has found limited use as a pharmacological or nutraceutical agent, which can be partly attributed to its low water-solubility and poor oral bioavailability.

Many efforts have been made to increase the water-dispersibility and bioavailability of curcumin, including encapsulation in liposomes (Dhule et al., 2012), cyclodextrins (Mohan et al., 2012), emulsions (Ahmed et al., 2012; Li, Ma, & Cui, 2014; Lin et al., 2009), solid lipid nanoparticles (Sun et al., 2013), polymer nanoparticles (Simion et al., 2013; Verderio et al., 2013), and inorganic nanoparticles (Gangwar et al., 2013; Jambhrunkar et al., 2014; Singh et al., 2013). Recently, there has been interest in utilizing biopolymer nanoparticles fabricated from proteins or polysaccharides to encapsulate curcumin, such as casein (Esmaili et al., 2011; Pan, Zhong, & Baek, 2013), chitosan (Yadav et al., 2012), and starch (Chin et al., 2014). The advantage of using food-grade biopolymers to fabricate delivery systems is that they can be incorporated into a wide range of commercial products, and they are biodegradable, natural, and label friendly.

Zein is the major storage protein in corn and consists of four major constituents: α-, β-, γ-, and δ-zein (Rishi & Munir, 2001). More than 50% of the amino acid residues in zein are hydrophobic, which makes it one of the few proteins that can be solubilized in concentrated aqueous ethanol (60–90%) solutions but not in pure water (Dong, Padua, & Wang, 2013; Zhang, Luo, & Wang, 2011). This property makes zein a suitable material for development of colloidal delivery systems to encapsulate hydrophobic bioactive molecules, such as curcumin (Chen & Zhong, 2014; Patel et al., 2010, 2013; Zhong & Jin, 2009). However, zein particles often have poor stability to aggregation when exposed to environmental conditions commonly encountered in food and pharmaceutical products, such as certain pH ranges, high salt contents, and

* Corresponding author at: Department of Food Science, University of Massachusetts, Amherst, MA 01003, USA. Tel.: +1 (413) 545 1019; fax: +1 (413) 545 1262.
E-mail address: mcclements@foodsci.umass.edu (D.J. McClements).

http://dx.doi.org/10.1016/j.foodchem.2015.03.009
0308-8146/

thermal processing. Researchers have shown that food biopolymers (such as sodium caseinate) can be used to coat zein nanoparticles and thereby improve their stability to aggregation under certain conditions (Patel et al., 2010).

Zein-biopolymer nanoparticles have already been used to encapsulate a variety of lipophilic bioactives, including α-tocopherol (Luo et al., 2011), vitamin D_3 (Luo, Teng, & Wang, 2012), and thymol (Zhang et al., 2014). In this study, we focus on the utilization of an anionic polysaccharide to coat and stabilize zein nanoparticles since this type of biopolymer is already widely used as a functional ingredient in the food industry. Previously, we have shown that alginate can be used to form core–shell zein-biopolymer nanoparticles with relatively small sizes (diameter = 150 nm), which had good stability over a range of temperatures, pH values, and ionic strengths (Hu & McClements, 2015). In the current study, we investigated the ability of citrus pectin to form and stabilize curcumin-loaded zein nanoparticles that might be suitable for use as delivery systems in the food and pharmaceutical industries.

2. Materials and methods

2.1. Materials

Zein (Lot SLBD5665V) was purchased from Sigma–Aldrich (St. Louis, MO, USA). Curcumin (>98%) was obtained from Acros Organics (New Jersey, USA). Pectin (Genu® pectin from *citrus*, type USP/100) was a gift from CP Kelco US Inc. (Atlanta, USA). Other chemicals, such as sodium chloride, sodium hydroxide, hydrochloric acid, HPLC grade ethanol alcohol, and dimethyl sulfoxide (DMSO), were obtained from Fisher Scientific (Fairlawn, NJ, USA).

2.2. Solution preparation

2.2.1. Curcumin–zein solution

1.7 g zein was added to 100.0 ml 85% (v/v) aqueous ethanol solution with magnetic stirring at 500 rpm (IKA R05) for 1 h, then curcumin powder was added and the mixture was stirred continuously for another hour.

2.2.2. Pectin solution

Pectin powder was dispersed in double distilled water at a concentration of 0.1% (w/v), and stirred for 3 h, then filtered through filter paper (Fisher Science, P5) to remove any insoluble components.

2.3. Preparation of curcumin loaded zein–pectin nanoparticles

5.88 ml of curcumin–zein ethanol solution was rapidly dropped into 25.00 ml of pH 4.0 adjusted water using a syringe with constant stirring at 900 rpm (IKA R05, USA). The resulting dispersion was then stirred for another 5 min, and then the ethanol was evaporated using a rotary evaporator (Rotavapor R110, Büchi Crop., Switzerland). Water (adjusted to pH 4.0) was added to compensate for the lost ethanol, so that the final volume of the dispersion was 25.00 ml. The dispersion was then filtered and poured into a 31.25 ml pectin solution with continuous stirring at 600 rpm for 30 min.

2.4. Nanoparticle characterization

2.4.1. Particle size and zeta potential measurements

The particle size distribution of the colloidal dispersions formed was measured by dynamic light scattering (DLS), Nano-ZS (Malvern Instruments, Worcestershire, UK). The Z-average diameter and polydispersity index (PDI) were calculated from the light scattering measurements. The electrical characteristics (ζ-potential) of the particles in the colloidal dispersions were determined using a micro-electrophoresis device (Nano-ZS, Malvern Instruments, Worcestershire, UK). Samples were diluted with water (adjusted to pH 4.0) prior to measurements to avoid multiple scattering effects.

2.4.2. Particle yield and curcumin loading efficiency (LE)

Freshly prepared colloidal dispersions were centrifuged at 3000 rpm for 10 min (Sorvall® RC-6 Plus, Thermo Electron Corporation, USA) to separate any large particles, and then the nanoparticles in the serum phase were freeze dried and weighed, and the curcumin content in the dried nanoparticles was determined. The particle yield and the curcumin loading efficiency were calculated as follows:

$$\text{Particle yield } (\%) = \frac{\text{the weight of the freeze dried particles}}{\text{total weight of curcumin, zein and pectin}} \times 100\% \quad (1)$$

$$\text{Loading efficiency } (\%) = \frac{\text{curcumin in nanoparticles}}{\text{total curcumin input}} \times 100\% \quad (2)$$

2.4.3. Curcumin loading determination

10 mg of freeze-dried nanoparticles were solubilized in 10 ml DMSO and then stirred overnight in the dark. The resulting solution was then centrifuged at 15,000 rpm for 30 min. The supernatant was diluted 10 times with DMSO, and the absorbance at $\lambda_{435\ nm}$ was measured using a UV-spectrophotometer (Ultrospec® 3000 Pro, Biochrom Ltd, England) to determine the curcumin concentration on the basis of a calibration curve which was previously established using standard solutions (0–10 μg/ml free curcumin in DMSO).

2.4.4. Transmission electron microscopy (TEM)

Freshly prepared colloid dispersions were diluted with water (adjusted to pH 4.0), then dropped onto a plasma-treated (glow-discharged) carbon-filmed grid and allowed to dry in the air. TEM experiments were performed on a JEM-2200FS microscope (JEOL Ltd, Japan) with an acceleration voltage of 200 kV. The image was taken on film at 20,000 × magnification.

2.5. Differential scanning calorimetry (DSC)

The thermal behavior of the dried nanoparticle sample was characterized using a differential scanning calorimeter (Q100, TA Instruments, USA). Ten milligrams of powdered sample were sealed in a hermetic aluminum pan and heated from 30 to 200 °C at a rate of 5 °C/min. Nitrogen was used as the transfer gas at a flow rate of 50 ml/min. Curcumin, zein, and pectin were also analyzed for comparison.

2.6. Fourier transform infrared spectroscopy (FTIR)

FTIR spectra of curcumin, zein, pectin, curcumin encapsulated nanoparticles, and curcumin–zein–pectin physical mixtures were recorded on a FTIR spectrophotometer (IR Prestige 21®, Shimadzu Corporation, Kyoto, Japan). The scanning range used was 600–1800 cm^{-1} with 32 scans and the resolution was set at 4 cm^{-1}.

2.7. Raman spectroscopy

A Raman microscope with spectroscopy capabilities (DXR Raman, Thermo Fisher Scientific, Madison, WI) was used to measure the spectra of curcumin, curcumin-encapsulated nanoparticles, and curcumin–zein–pectin physical mixtures. This instrument used

780 nm excitation and 24 mW laser power through a 10 × objective (Olympus, Japan). The aperture was set at 50 μm slit, grating 400 lines/mm, and spot size of 3.1 μm. The collection exposure time was 1.0 s and the sample exposure was 2.0 s. The working distance of the objective lens to the surface of the gold slide was kept constant at 6.5 mm to minimize variance. At least 15 spectra were recorded per sample and each sample was analyzed 3 times. The mean spectral data were then analyzed using instrument software (TQ analyst, Thermo Fisher Scientific).

2.8. Dispersibility characterization

The water-dispersibility of the dried core–shell nanoparticles was determined by dispersing 5 mg of powdered nanoparticles in 25 ml double distilled water with constant stirring at 700 rpm for 3 h. The visual appearance of the resulting colloidal dispersions was then recorded using a digital camera. The particle size and PDI were measured by dynamic light scattering (Nano-ZS, Malvern Instruments, Worcestershire, UK).

2.9. Data analysis

All experiments were carried out at least twice and the results were reported as averages and standard deviations of these measurements. Means were subjected to Duncan's test and a p-value of <0.05 was considered statistically significant.

3. Results and discussion

3.1. Nanoparticle size, ζ-potential and morphology

Zein-pectin nanoparticles containing different added curcumin contents ranging from 0.88% to 9.46% were synthesized. The mean particle diameter (≈250 nm), polydispersity index (≈0.24), and ζ-potential (≈−28 mV) of the nanoparticles measured at pH 4 were not strongly affected by curcumin content (Table 1). These results suggest that the curcumin was contained inside the particles and did not have a strong impact on their formation or surface properties. The negative charge on the zein-pectin nanoparticles is indicative of their core–shell structure, and is a result of adsorption of anionic pectin molecules onto the surfaces of cationic zein molecules. Indeed, the ζ-potential at pH 4 of a pectin solution was determined to be −34 mV, whereas that of bare curcumin-fortified zein nanoparticles was +31 mV. Zein has been reported to have an isoelectric point (pI) around pH 6.2 (Rishi & Munir, 2001), while the carboxyl groups on pectin have been reported to have a dissociation constant (pK_a) around pH 3.5 (Jones et al., 2010). At pH 4.0, the zein molecules should therefore have a net positive charge, while the pectin molecules should have a net negative charge. The adsorption of the pectin molecules to the zein particle surfaces can therefore be attributed to electrostatic attraction between these two biopolymers at this pH. The fact that the net charge on the nanoparticles was negative is due to the fact that the pectin molecules formed the outer coating, and not all of the anionic groups on the pectin molecules were bound to cationic groups on the zein nanoparticles.

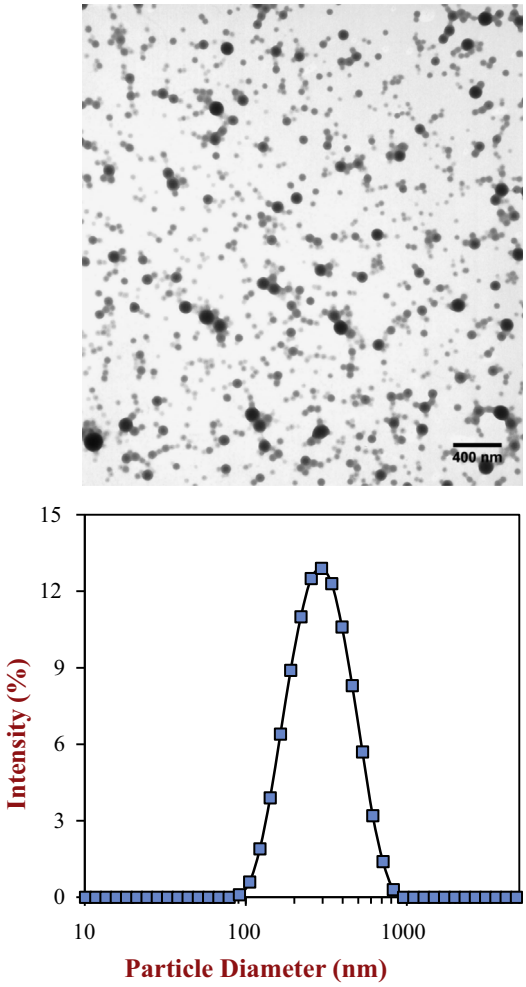

Fig. 1. TEM image and particle size distribution of curcumin-loaded zein-pectin nanoparticles (pH 4). The curcumin content in the particles was 4.63% (w/w).

Transmission electron microscopy analysis showed that the nanoparticles were spherical with smooth surfaces (Fig. 1). Most of the particles in the TEM images had diameters in the range 100 to 200 nm, but there were also some smaller particles. The particle size observed by TEM was therefore somewhat smaller than that determined by DLS, which measured an average mean particle diameter of 250 nm (Fig. 1). This may be explained by the fact that most of the water in the nanoparticles was evaporated within the high vacuum chamber of the TEM instrument, which resulted in some particle shrinkage.

3.2. Curcumin loading characteristics

The yields of curcumin-fortified nanoparticles collected after the fabrication process were always relatively high, ranging from around 92% to 97% (Table 1), which indicated that the particle preparation method was efficient. No large particles were observed by

Table 1
Particle size, charge, yield and loading efficiencies of curcumin-fortified zein-pectin nanoparticles. The theoretical curcumin content is the amount added originally.

Theoretical curcumin content (%)	ζ-Potential (mV)	Mean particle diameter (nm)	PDI	Determined curcumin content (%)	Particle yield (%)	Curcumin loading efficiency (%)
0.88	−27.9 ± 0.9	250.2 ± 7.3	0.235 ± 0.007	0.84 ± 0.01	96.5 ± 2.1	91.8 ± 1.1
2.39	−27.2 ± 0.8	244.0 ± 8.5	0.232 ± 0.006	2.25 ± 0.03	96.3 ± 1.3	90.8 ± 1.1
4.63	−28.7 ± 1.4	245.7 ± 6.5	0.232 ± 0.014	4.25 ± 0.08	93.7 ± 3.0	86.0 ± 1.7
7.27	−26.9 ± 1.2	252.9 ± 4.4	0.252 ± 0.008	6.76 ± 0.16	92.7 ± 1.1	86.2 ± 2.0
9.46	−28.1 ± 1.8	250.3 ± 11.2	0.248 ± 0.004	8.80 ± 0.19	93.4 ± 0.5	86.8 ± 1.9

eye in the samples during the particle fabrication process, which accounts for the high particle yield. The curcumin contents measured in the freeze-dried nanoparticles were also relatively high (86–92%), with the loading efficiency decreasing slightly with increasing curcumin concentration.

3.3. Differential scanning calorimetry

The DSC profiles for curcumin in pure form, in a physical mixture with pectin and zein, and encapsulated within zein-pectin nanoparticles are shown in Fig. 2. In the pure curcumin, there was a sharp endothermic peak around 177 °C, which has previously been attributed to melting of curcumin crystals (Mohan et al., 2012; Pan et al., 2013). In the physical mixtures there was a broad endothermic peak around 136 °C and a sharp endothermic peak around 176 °C. The broad peak can be attributed to water evaporation from powdered pectin (Wang, Chen, & Lü, 2014), whereas the sharp peak corresponds to the melting of curcumin crystals (Mohan et al., 2012; Pan et al., 2013), which suggests that the curcumin was in a crystalline form in the physical mixtures. The fact that the peak was much smaller in the physical mixture than in the pure curcumin can be attributed to the fact that the mixture only contained 7.27% curcumin. In the powdered system containing curcumin-fortified zein-pectin nanoparticles there was no evidence of a sharp endothermic peak around 177 °C, which suggests that the curcumin was in an amorphous form, rather than in a crystalline form. Presumably, the curcumin molecules were intimately mixed with the zein molecules inside the nanoparticles. Amorphous curcumin has also been reported in zein nanoparticles and casein nanoparticles by X-ray diffraction (Esmaili et al., 2011; Pan et al., 2013).

3.4. FTIR spectrometry

Fourier transform infrared measurements were used to provide some information about the nature of the interactions inside the nanoparticles. FTIR peak assignments for the different spectra are presented in Figs. 3a and 3b and Table 2. In the curcumin spectrum, there were no peaks in the most significant carbonyl region (1800–1650 cm^{-1}), indicating that curcumin existed in the keto-enol tautomeric form (Mangolim et al., 2014). In the physical mixture and nanoparticles, the peaks at 1626, 1600, 1506 cm^{-1} observed in pure curcumin were masked by the amide I and amide II bands from the zein. Since the pectin content was only 20% in the physical mixture and nanoparticles, its FTIR signal was too low to be detected in these spectra. The peaks at 1273 cm^{-1} observed in the spectra of pure curcumin and the physical mixture were assigned to δ(CCC) and δ(CCH) of the aromatic "keto" part, and δ(COH) of the "keto" part of curcumin (Kolev, Velcheva, Stamboliyska, & Spiteller, 2005). This peak was shifted to 1278 cm^{-1} in the spectrum of the curcumin-fortified zein-pectin nanoparticles. The peak at 1113 cm^{-1} was assigned to υ(O—CH_3), δ(CCH) of aromatic rings in the pure curcumin (Kolev et al., 2005), which shifted to 1103 cm^{-1} in the nanoparticles. The peak of 1026 cm^{-1} was assigned to $\gamma(CH_3)$ and δ(CCH) of aromatic ring connected with the "enolic" part of curcumin (Kolev et al., 2005), which shifted to 1018 cm^{-1} in the nanoparticles.

The peaks at 1427, 1185, 1154 cm^{-1} were related to the vibrations of δ(CCC), δ(CCH), and δ(C—O—C) of aromatic rings and the inter-ring chain of pure curcumin (Kolev et al., 2005; Vu et al., 2009). Interestingly, these peaks were not observed in the spectrum of the curcumin-fortified nanoparticles. The peaks at 885, 855, and 808 cm^{-1} were assigned toγ(CCH) of aromatic ring connected with "enolic" part of the curcumin molecule, γ(CCH) of aromatic rings and inter-ring chain, and γ(CCH) of aromatic ring connected with "keto" part of the molecule respectively (Kolev et al., 2005), and also disappeared from the spectrum of nanoparticles.

The changes of the FTIR signals relating to the vibrations of aromatic rings and inter-ring chain of the encapsulated curcumin suggested that these hydrophobic groups interacted with zein proteins possibly by hydrophobic interactions.

The υ(C—O), δ(COH) connected to aromatic rings, and δ(COH) of enolic form were also changed since the related peaks at

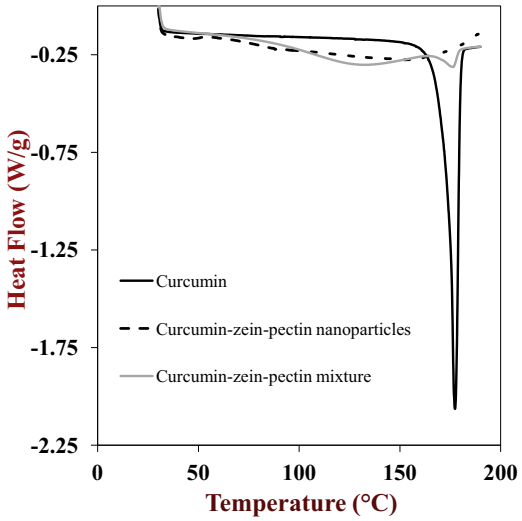

Fig. 2. DSC profiles (heat flow *versus* temperature) of curcumin in different forms: pure curcumin: curcumin encapsulated within zein-pectin nanoparticles; curcumin mixed with zein and pectin (physical mixture). The curcumin content was 7.27 %(w/w) in the nanoparticles and mixture.

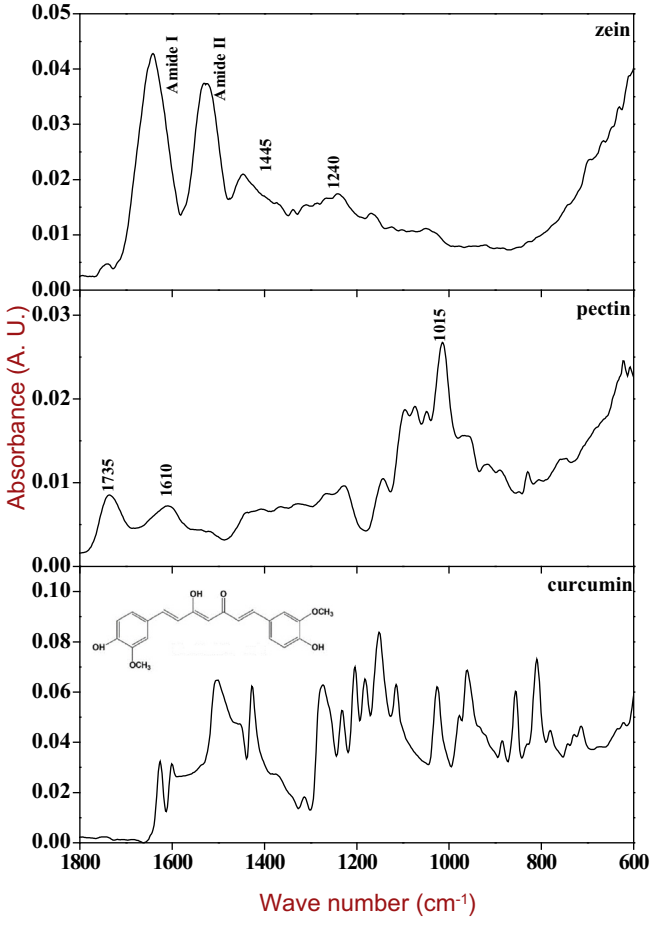

Fig. 3a. FTIR spectra of pure curcumin, pectin, and zein powders.

1313 cm^{-1} and 1233 cm^{-1} disappeared in the spectrum of the nanoparticles. These disappearances suggested that hydrophilic groups may also interact with zein proteins possibly by H-bonding, or the curcumin molecular conformation might be changed from the enolic form to diketo form.

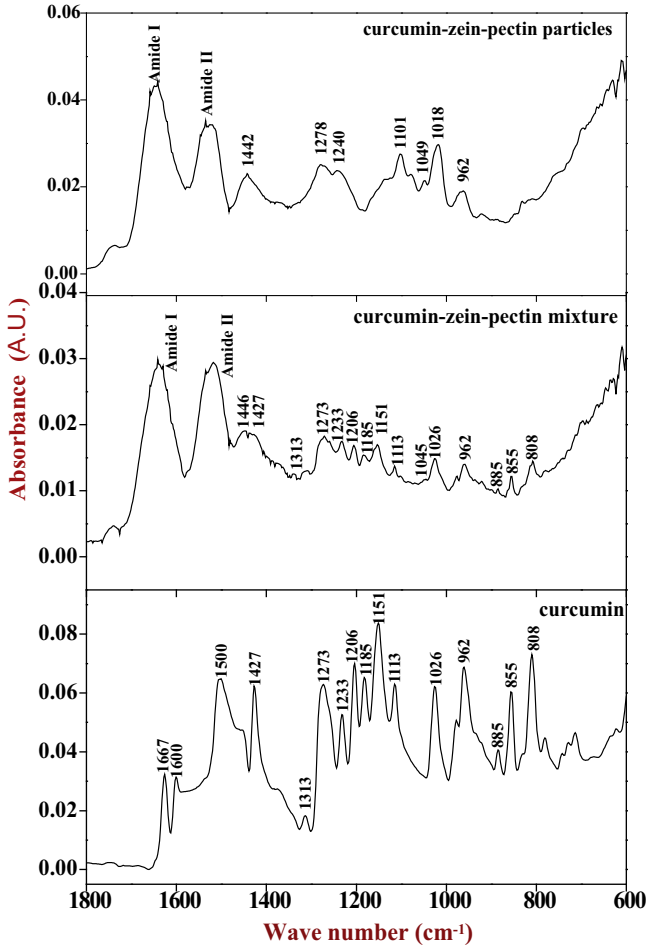

Fig. 3b. FTIR spectra of curcumin, curcumin-zein-pectin mixture, and curcumin-zein-pectin nanoparticles (curcumin content was 9.46% in mixture and particles (w/w)).

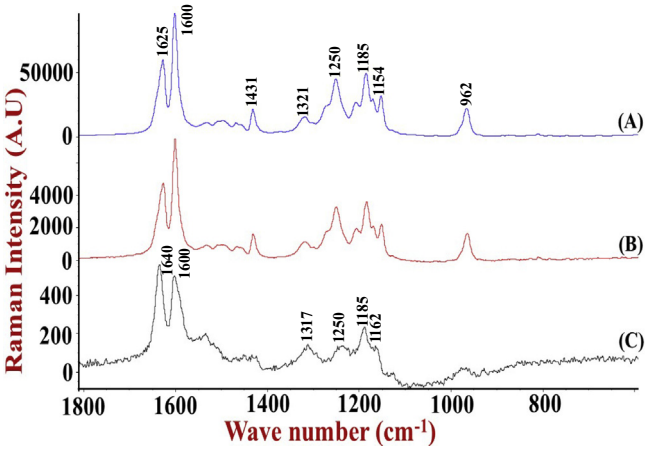

Fig. 3c. Raman spectra of curcumin (A), curcumin-zein-pectin mixture (B), and curcumin-zein-pectin nanoparticles (C), curcumin content was 7.27% in mixture and particles (w/w).

3.5. Raman spectroscopy

Raman spectroscopy was used to provide additional information about the molecular interactions in the systems. The Raman spectra of curcumin, zein-pectin-curcumin physical mixtures, and curcumin-fortified zein-pectin nanoparticles are shown in Fig. 3c and Table 2. The spectra of pure zein and pectin were not included because their Raman intensities were too weak. The peak at 1625 cm^{-1} was attributed to the υ(C=C) and υ (C=O) of inter-ring chain in curcumin spectrum, and the peak at 1600 cm^{-1} was attributed to the C=C stretching of curcumin aromatic rings (Mangolim et al., 2014; Mohan et al., 2012). These bands were unchanged in the spectrum of the physical mixtures, but the peak at 1625 cm^{-1} in the mixture spectrum shifted to 1640 cm^{-1} in nanoparticle spectrum, and the intensity of the peak at 1600 cm^{-1} in the nanoparticle spectrum decreased appreciably when compared to that of the mixture spectrum. These changes indicated that the aromatic rings and inter-ring chain of curcumin all interacted with zein. Similar changes were observed in curcumin/cyclodextrin complexes, where it was suggested that the aromatic rings were encapsulated in the hydrophobic cavity of cyclodextrins (Mangolim et al., 2014; Mohan et al., 2012).

Table 2
FTIR and Raman spectrum peak assignments of free curcumin, mixture, and nanoparticles [a].

Curcumin (cm^{-1})		Curcumin in mixture (cm^{-1})		Curcumin in nanoparticles (cm^{-1})		Peak assignments[b]
FTIR	Raman	FTIR	Raman	FTIR	Raman	
1626	1625	–	1625	–	1640	υ(C=C) and υ(C=O) of the inter-ring chain
1600	1600	–	1600	–	1600	υ(C=C) of aromatic rings
1506		–		–		υ(C=O), δCCC, δCC=O
1427	1431	1427	1431	–	1431	δ(CCC), δ(CCH), and δ(COH)of aromatic rings
1313	1321	1313	1321	–	1317	υ(C—O)
1273		1273		1278		δ(CCC) and δ(CCH) of aromatic "keto" part, δ(COH) of "keto" part
	1250		1250		1250	δ(CH) of the aromatic rings, associated to υ(C—O) of the ether groups linked to these rings
1233		1233		–		δ(COH) connected to aromatic rings, δ(COH) of enolic form
1205		1205		–		δ(CCH)
1185	1185	1185	1185	–	1185	δ(C—O—C)
1151	1154	1151	1154	–	1162	δ(CCH) of aromatic rings, δ(CCH) of inter-ring chain
1113		1113		1103		υ(O—CH_3), δ(CCH) of aromatic ring connected to "enolic" part
1026		1026		1018		υ(C—O—C), δ(CCH) of aromatic ring connected with "enolic" part, γ(CH_3)
962	962	962	962	962	–	υ(C^{12}O), δ(C^{12}OH)
885		885		–		γ(CCH) of aromatic ring connected with "enolic" part of the molecule
855		855		–		γ(CCH)of aromatic rings and inter-ring chain
808		808		–		γ(CCH) of aromatic ring connected with "keto" part of the molecule

[a] cited from Bich et al. (2009), Kolev et al. (2005), López-Tobar et al. (2012), Mangolim et al. (2014) and Mohan et al. (2012).
[b] Vibration modes: υ, stretching; δ, in-plane bending; γ, out-of-plane bending.

The peak at 1431 cm^{-1} in the curcumin spectrum was assigned to δ(CCC), δ(COH), and δ(CCH) of aromatic rings (Kolev et al., 2005), and the peak at 1250 cm^{-1} was attributed to the δ(CH) of the aromatic rings, combined to υ(C—O) of the ether groups linked to these rings (Mangolim et al., 2014). The intensities of these two peaks decreased in the spectrum of the nanoparticles when compared to those in the mixture spectrum even though both of them contained equal amounts of curcumin. The peak of 1154 cm^{-1} in the mixture spectrum, which was assigned to δ(CCH) of aromatic rings, δ(CCH) of the inter-ring chain (Kolev et al., 2005), shifted to 1162 cm^{-1} in the spectrum of the nanoparticles. These differences also suggested that the aromatic rings on the curcumin interacted with the zein molecules through hydrophobic interactions.

The peak at 1321 cm^{-1} was assigned to υ(C—O) in pure curcumin (Vu et al., 2009), which shifted to 1316 cm^{-1} in the nanoparticles. The peak at 962 cm^{-1} in the mixture spectrum was assigned to the stretching of enolic C^{12}-O and the in plane bending of $C^{12}OH$ (Kolev et al., 2005), and totally disappeared in the nanoparticle spectrum. Other researchers have also reported that the intensity of the peak at 962 cm^{-1} decreased when curcumin was encapsulated in cyclodextrins, and attributed this to isomerization from the keto-enol to the diketo form (López-Tobar, Blanch, Ruiz del Castillo, & Sanchez-Cortes, 2012). It has been suggested that free curcumin crystallizes in an enol form stabilized by strong intramolecular H-bonds (Kolev et al., 2005). The disappearance of the peak at 962 cm^{-1} in the nanoparticles suggests that an isomerization from the keto-enol to the diketo form of curcumin occurred when it was encapsulated within a zein matrix, and that H-bonds could not form between the diketo isomers, which prevented curcumin crystalizing. Moreover, the diketo isomer was less polar than the enol-keto one and easier to form hydrophobic interactions with zein.

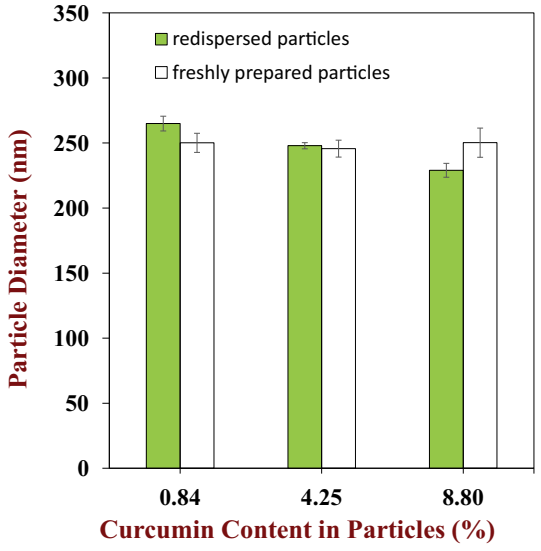

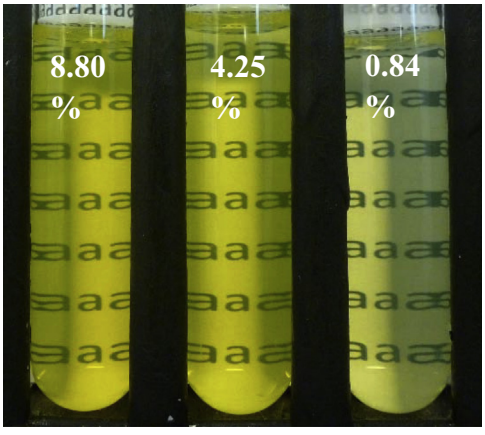

Fig. 4. Mean particle diameters of freshly prepared and redispersed freeze-dried nanoparticles. The photograph is of the redispersed nanoparticles in double distilled water at a concentration of 0.2 mg/ml.

3.6. Redispersibility of nanoparticles

Freeze-dried nanoparticles were redispersed in double distilled water with stirring, and then their appearance was recorded (Fig. 4). The colloidal dispersions had a clear yellow appearance with the intensity of the color increasing with curcumin content. The average diameter of the redispersed nanoparticles was in the range 229 to 265 nm and decreased slightly with increasing curcumin content ($p < 0.05$). These values are fairly similar to those of the freshly prepared nanoparticles ($d \approx 250$ nm). The polydispersity of the redispersed nanoparticles and freshly prepared nanoparticles were both in the range 0.23 to 0.25. These results suggest that the freeze-drying and rehydration process did not promote particle aggregation. Consequently, it is possible to dehydrate the zein-pectin nanoparticles for utilization as powdered functional ingredients in foods and beverages.

4. Conclusions

We successively prepared core–shell biopolymer particles by coating cationic zein nanoparticles with anionic pectin molecules using an electrostatic deposition method. These nanoparticles were able to encapsulate appreciable quantities of curcumin at a high loading efficiency (>86%). The core–shell particles formed were relatively small ($d \approx 250$ nm) and had a uniform spherical shape. The encapsulated curcumin was shown to be in an amorphous form by DSC, which may be advantageous since studies in the pharmaceutical industry have shown that amorphous drugs have higher bioavailability than crystalline ones. FTIR and Raman spectroscopy suggested that the encapsulated curcumin interacted with the zein matrix primarily through hydrophobic interactions. The nanoparticles could be converted into a powdered form that could easily be redispersed in water leading to the formation of a transparent liquid. Consequently, the core–shell nanoparticles developed in this study may be suitable for application in functional food and beverage products.

References

Ahmed, K., Li, Y., McClements, D. J., & Xiao, H. (2012). Nanoemulsion- and emulsion-based delivery systems for curcumin: Encapsulation and release properties. *Food Chemistry, 132*(2), 799–807.

Anand, P., Kunnumakkara, A. B., Newman, R. A., & Aggarwal, B. B. (2007). Bioavailability of curcumin-Problems and promises. *Molecular Pharmaceutics, 4*(6), 807–818.

Anand, P., Thomas, S. G., Kunnumakkara, A. B., Sundaram, C., Harikumar, K. B., Sung, B., et al. (2008). Biological activities of curcumin and its analogues (Congeners) made by man and Mother Nature. *Biochemistry and Pharmacology, 76*(11), 1590–1611.

Bhawana Basniwal, R. K., Buttar, H. S., Jain, V. K., & Jain, N. (2011). Curcumin nanoparticles: Preparation, characterization, and antimicrobial study. *Journal of Agriculture and Food Chemistry, 59*, 2056–2061.

Bich, V. T., Thuy, N. T., Binh, N. T., Huong, N. T. M., Yen, P. N. D., & Luong, T. T. (2009). Structural and Spectral Properties of Curcumin and Metal- Curcumin Complex Derived from Turmeric (Curcuma longa). In D. T. Cat, A. Pucci & K. Wandelt (Eds.), Physics and Engineering of New Materials, (pp. 271–278).

Chen, H., & Zhong, Q. (2014). Processes improving the dispersibility of spray-dried zein nanoparticles using sodium caseinate. *Food Hydrocolloids, 35*, 358–366.

Chin, S. F., Mohd, Y., Siti, N. A., & Pang, A. C. (2014). Preparation and characterization of starch nanoparticles for controlled release of curcumin. *International Journal of Polymer Science, 2014*, 1–8.

Dhule, S. S., Penfornis, P., Frazier, T., Walker, R., Feldman, J., Tan, G., et al. (2012). Curcumin-loaded gamma-cyclodextrin liposomal nanoparticles as delivery vehicles for osteosarcoma. *Nanomedicine, 8*(4), 440–451.

Dong, F., Padua, G. W., & Wang, Y. (2013). Controlled formation of hydrophobic surfaces by self-assembly of an amphiphilic natural protein from aqueous solutions. *Soft Matter, 9*(25), 5933.

Duvoix, A., Blasius, R., Delhalle, S., Schnekenburger, M., Morceau, F., Henry, E., et al. (2005). Chemopreventive and therapeutic effects of curcumin. *Cancer Letters, 223*(2), 181–190.

Esmaili, M., Ghaffari, S. M., Moosavi-Movahedi, Z., Atri, M. S., Sharifizadeh, A., Farhadi, M., et al. (2011). Beta casein-micelle as a nano vehicle for solubility enhancement of curcumin; food industry application. *LWT – Food Science and Technology, 44*(10), 2166–2172.

Gangwar, R. K., Tomar, G. B., Dhumale, V. A., Zinjarde, S., Sharma, R. B., & Datar, S. (2013). Curcumin conjugated silica nanoparticles for improving bioavailability and its anticancer applications. *Journal of Agriculture and Food Chemistry, 61*(40), 9632–9637.

Hu, K., & McClements, D. J. (2015). Fabrication of biopolymer nanoparticles by antisolvent precipitation and electrostatic deposition: Zein-alginate core/shell nanoparticles. *Food Hydrocolloids, 44*, 101–108.

Jambhrunkar, S., Karmakar, S., Popat, A., Yu, M., & Yu, C. (2014). Mesoporous silica nanoparticles enhance the cytotoxicity of curcumin. *RSC Advances, 4*(2), 709.

Jones, O. G., Lesmes, U., Dubin, P., & McClements, D. J. (2010). Effect of polysaccharide charge on formation and properties of biopolymer nanoparticles created by heat treatment of β-lactoglobulin–pectin complexes. *Food Hydrocolloids, 24*, 374–383.

Kolev, T. M., Velcheva, E. A., Stamboliyska, B. A., & Spiteller, M. (2005). DFT and experimental studies of the structure and vibrational spectra of curcumin. *International Journal of Quantum Chemistry, 102*, 1069–1079.

Kumar, S. S., Mahesh, A., Mahadevan, S., & Mandal, A. B. (2014). Synthesis and characterization of curcumin loaded polymer/lipid based nanoparticles and evaluation of their antitumor effects on MCF-7 cells. *Biochimica Biophysica Acta, 1840*(6), 1913–1922.

Li, M., Ma, Y., & Cui, J. (2014). Whey-protein-stabilized nanoemulsions as a potential delivery system for water-insoluble curcumin. *LWT – Food Science and Technology, 59*(1), 49–58.

Lin, C. C., Lin, H. Y., Chen, H. C., Yu, M. W., & Lee, M. H. (2009). Stability and characterisation of phospholipid-based curcumin-encapsulated microemulsions. *Food Chemistry, 116*, 923–928.

López-Tobar, E., Blanch, G. P., Ruiz del Castillo, M. L., & Sanchez-Cortes, S. (2012). Encapsulation and isomerization of curcumin with cyclodextrins characterized by electronic and vibrational spectroscopy. *Vibrational Spectroscopy, 62*, 292–298.

Luo, Y., Teng, Z., & Wang, Q. (2012). Development of zein nanoparticles coated with carboxymethyl chitosan for encapsulation and controlled release of vitamin D3. *Journal of Agriculture and Food Chemistry, 60*(3), 836–843.

Luo, Y., Zhang, B., Whent, M., Yu, L. L., & Wang, Q. (2011). Preparation and characterization of zein/chitosan complex for encapsulation of alpha-tocopherol, and its in vitro controlled release study. *Colloids and Surfaces B, 85*(2), 145–152.

Mangolim, C. S., Moriwaki, C., Nogueira, A. C., Sato, F., Baesso, M. L., Neto, A. M., et al. (2014). Curcumin-beta-cyclodextrin inclusion complex: Stability, solubility, characterisation by FT-IR, FT-Raman, X-ray diffraction and photoacoustic spectroscopy, and food application. *Food Chemistry, 153*, 361–370.

Mohan, P. R. K., Sreelakshmi, G., Muraleedharan, C. V., & Joseph, R. (2012). Water soluble complexes of curcumin with cyclodextrins: Characterization by FT-Raman spectroscopy. *Vibrational Spectroscopy, 62*, 77–84.

Pan, K., Zhong, Q., & Baek, S. J. (2013). Enhanced dispersibility and bioactivity of curcumin by encapsulation in casein nanocapsules. *Journal of Agriculture and Food Chemistry, 61*(25), 6036–6043.

Patel, A. R., Heussen, P. C., Dorst, E., Hazekamp, J., & Velikov, K. P. (2013). Colloidal approach to prepare colour blends from colourants with different solubility profiles. *Food Chemistry, 141*(2), 1466–1471.

Patel, A. R., Hu, Y., Tiwari, J. K., & Velikov, K. P. (2010). Synthesis and characterisation of zein–curcumin colloidal particles. *Soft Matter, 6*(24), 6192.

Rishi, S., & Munir, C. (2001). Zein the industrial protein from corn. *Industrial Crops and Products, 13*, 171–192.

Simion, V., Stan, D., Gan, A.-M., Pirvulescu, M. M., Butoi, E., Manduteanu, I., et al. (2013). Development of curcumin-loaded poly(hydroxybutyrate-co-hydroxyvalerate) nanoparticles as anti-inflammatory carriers to human-activated endothelial cells. *Journal of Nanoparticle Research, 15*(12).

Singh, D. K., Jagannathan, R., Khandelwal, P., Abraham, P. M., & Poddar, P. (2013). In situ synthesis and surface functionalization of gold nanoparticles with curcumin and their antioxidant properties: An experimental and density functional theory investigation. *Nanoscale, 5*(5), 1882–1893.

Sun, J., Bi, C., Chan, H. M., Sun, S., Zhang, Q., & Zheng, Y. (2013). Curcumin-loaded solid lipid nanoparticles have prolonged in vitro antitumour activity, cellular uptake and improved in vivo bioavailability. *Colloids and Surfaces B, 111*, 367–375.

Verderio, P., Bonetti, P., Colombo, M., Pandolfi, L., & Prosperi, D. (2013). Intracellular drug release from curcumin-loaded PLGA nanoparticles induces G2/M block in breast cancer cells. *Biomacromolecules, 14*(3), 672–682.

Vu, T. B., Nguyen, T. T., Nguyen, T. B., Nguyen, T. M. H., Pham, N. D. Y., & Tran, T. L. (2009). Structural and Spectral Properties of Curcumin and Metal- Curcumin Complex Derived from Turmeric (Curcuma longa). In D. T. Cat, A. Pucci & K. Wandelt (Eds.), Physics and Engineering of New Materials, (pp. 271–278).

Wang, X., Chen, Q., & Lü, X. (2014). Pectin extracted from apple pomace and citrus peel by subcritical water. *Food Hydrocolloids, 38*, 129–137.

Yadav, A., Lomash, V., Samim, M., & Flora, S. J. (2012). Curcumin encapsulated in chitosan nanoparticles: A novel strategy for the treatment of arsenic toxicity. *Chemico-Biological Interactions, 199*(1), 49–61.

Zhang, B., Luo, Y., & Wang, Q. (2011). Effect of acid and base treatments on structural, rheological, and antioxidant properties of α-zein. *Food Chemistry, 124*(1), 210–220.

Zhang, Y., Niu, Y., Luo, Y., Ge, M., Yang, T., Yu, L. L., et al. (2014). Fabrication, characterization and antimicrobial activities of thymol-loaded zein nanoparticles stabilized by sodium caseinate-chitosan hydrochloride double layers. *Food Chemistry, 142*, 269–275.

Zhong, Q., & Jin, M. (2009). Zein nanoparticles produced by liquid–liquid dispersion. *Food Hydrocolloids, 23*(8), 2380–2387.